

If we assume that the viscosity isotherms retain their linearity for an even deeper penetration into the metastable region, we may approximate the viscosity for the states of accessible superheating of the liquids by the line 3 in Fig. 2. The region of metastable (superheated) states lies between lines 2 and 3.

#### NOTATION

$\rho_{\text{Hg}}$ ,  $\rho$ , densities of mercury at room temperature and the liquid under consideration at the thermostat temperature, respectively;  $g$ , gravitational acceleration;  $h$ , distance from the mercury level in the glass vessel to that in the measuring tube (Fig. 1);  $h_1$ ,  $h_2$ , distances from the mercury level in the glass vessel to the lower and upper contacts, respectively;  $\tau$ , time for a specified volume of liquid  $V$  to pass through the capillary  $V$ ,  $V = 0.25 \pi d^2 (h_2 - h_1)$ ;  $d$ , internal diameter of the measuring tube;  $\eta$ , viscosity of the liquid under consideration;  $L$ , length;  $2r$ , diameter of the capillary;  $A$ , a quantity allowing for the nonisothermal nature of the flow of liquid through the capillary;  $P_s$ ,  $P_{\text{su}}$ , pressures of the saturated vapor and the greatest possible superheating of the liquid, respectively;  $T_C$ , critical temperature. Indices: 0, quantities corresponding to the reference pressure  $P_0$ .

#### LITERATURE CITED

1. V. E. Denny and R. Ferenbaugh, *J. Chem. Eng. Data*, **12**, 379 (1967).
2. I. F. Golubev and N. A. Agaev, *Viscosity of Saturated Hydrocarbons* [in Russian], Azerneshr, Baku (1964).
3. Yu. A. Aleksandrov et al., *Bubble Chambers* [in Russian], Gosatomizdat, Moscow (1963).
4. V. P. Skripov, *Metastable Liquid* [in Russian], Nauka, Moscow (1972).
5. P. I. Voskresenskii, *Fundamentals of Laboratory Technique* [in Russian], Khimiya, Moscow (1971).
6. N. B. Vargaftik, *Handbook on the Thermophysical Properties of Gases and Liquids* [in Russian], Nauka, Moscow (1972).

#### USE OF A MICROCALORIMETER OF THE CALVÉ TYPE FOR DETERMINING THE KINETIC CHARACTERISTICS OF THERMAL EFFECTS IN CHEMICALLY REACTING MATERIALS

B. A. Arutyunov, V. V. Vlasov,  
O. A. Gerashchenko, S. V. Mishchenko,  
and N. P. Puchkov

UDC 536.63.083

The construction of a dynamic microcalorimeter designed for measuring the kinetic characteristics of thermal effects in solid and powdered polymer materials which react chemically on heating is considered.

It is well known [1] that the kinetic characteristics of thermal effects in chemically interacting materials may be determined calorimetrically from the relationship between the rate of heat evolution by unit mass of the reacting mixture  $dQ/d\tau$  and the velocity  $d\varphi/d\tau$  of the corresponding reaction. However, the adiabatic-microcalorimeter method usually employed has the following shortcomings: the necessity of introducing a correction for heat exchange with the ambient, and the impossibility of determining the thermal effect of the reaction without a priori knowledge as to the specific heat of the test material, which is assumed to be an invariant function with respect to temperature. The use of the dynamic microcalorimeter considered in this paper overcomes these obstacles and reveals the influence of heating rate on the kinetic parameters of chemically reacting materials.

Translated from *Inzhenerno-Fizicheskii Zhurnal*, Vol. 29, No. 6, pp. 1080-1083, December, 1975. Original article submitted January 29, 1975.

*This material is protected by copyright registered in the name of Plenum Publishing Corporation, 227 West 17th Street, New York, N.Y. 10011. No part of this publication may be reproduced, stored in a retrieval system, or transmitted, in any form or by any means, electronic, mechanical, photocopying, microfilming, recording or otherwise, without written permission of the publisher. A copy of this article is available from the publisher for \$7.50.*

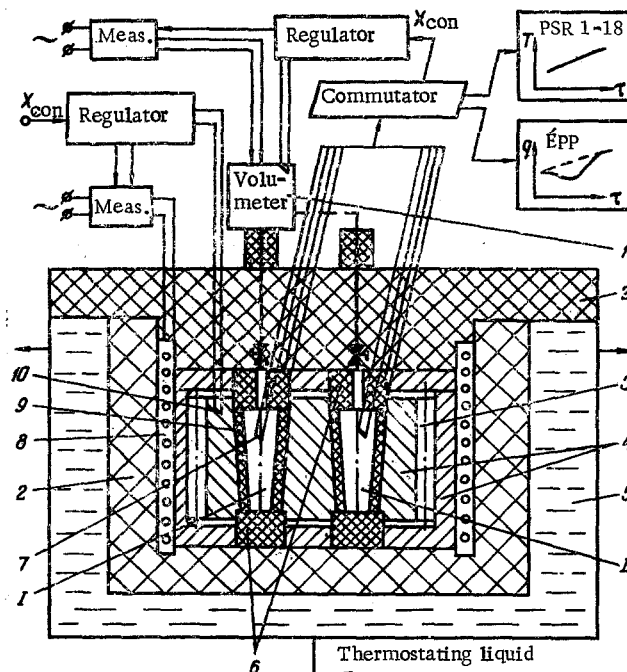


Fig. 1. Microcalorimetric apparatus for quantitatively determining the thermal effects of chemically reacting materials  $T$ , °C;  $q$ , W/m<sup>2</sup>,  $\tau$ , sec.

The microcalorimeter consists of two identical measuring elements I and II (Fig. 1) constituting copper sleeves containing copper-Constantan thermopiles 9, prepared by electrodeposition. The thermopiles are fixed in the sleeves and the sleeves themselves in the copper block 4 by means of a thin glue interlayer possessing a good thermal conductivity. Ground silver calorimetric vessels with an internal diameter of 5 mm are inserted into the copper sleeves. The electric signal of the differentially connected thermopiles is recorded with an ÉPP-17MZ automatic recorder, having eight measuring ranges, from 1 to 128 mV. At the same time a PSR-18 potentiometer records the temperature of the block and the measuring cells by means of the thermocouples 7 and 10. The temperature fluctuations of the heater 8 surrounding the measuring cells are partly stabilized by introducing an additional thermal resistance in the form of apertures 3 sited around the circumference of the copper block. In order to reduce the end losses, thermal insulation is provided in the form of Teflon stoppers 6 and glass-wool layers 2 enclosed in a thermostating screen 5. In order to eliminate the loss of heat by gas convection, an automatic control system is incorporated in the volumeter 1, keeping the temperature of the latter equal to the sample temperature. The temperature conditions are regulated by means of an appropriately positioned regulator built into the ÉPV-2-11A instrument.

The microcalorimeter was calibrated by means of a potentiometric system based on the Joule effect. The power  $dQ/d\tau$  was calculated from the Calvé-Tian equation [2]:

$$\frac{dQ}{d\tau} = k \left[ \Delta T + \tau_{\text{ins}} \frac{d\Delta T}{d\tau} \right], \quad (1)$$

where  $\Delta T$  is the deflection of the instrument needle in mm. For our present microcalorimeter the calibration constant with respect to the deflection  $k$  (the sensitivity of the instrument) equals 0.00203-0.26 W/mm (depending on the scale of the instrument), while  $\tau_{\text{ins}}$  (time constant of the instrument) equals 10-30 sec (depending on the mass and the thermophysical characteristics of the samples).

It should be noted that the sensitivity of the microcalorimeter may be greatly increased by using a photo-compensation amplifier of the F116/1 type.

The total thermal effect is determined by integrating the thermal power. A knowledge of the mass of the test material  $m$  enables us to determine the specific thermal effect of the reaction  $\Delta H = Q/m$ .

TABLE 1. Kinetic Characteristics of the Thermal Effects Involved in the Hardening and Vulcanization of Certain Polymer Materials

Material	Rate of rise, temperature °C/sec	Reaction parameter (effective)	Exponential index, deg · 10 <sup>-3</sup>	Decimal logarithm, k <sub>0</sub> , 1/sec	Temperature at the onset of the reaction, °C	Specific thermal effect of the reaction, J/g
Ebonite LI-10	0,0224	1,05	28,08	25,18	141,5	213,5
	0,0305	1,05	26,52	23,39	143,3	
	0,0438	1,075	22,73	19,37	145,0	
	0,0622	1,10	19,65	16,05	147,0	
	0,0801	1,125	17,81	14,11	148,8	
Ebonite ZV-8	0,0215	1,005	27,31	24,21	140,4	298,6
	0,0321	1,025	21,68	18,30	142,0	
	0,0462	1,05	18,34	14,75	143,0	
	0,0621	1,075	16,77	13,07	145,0	
SemiEbonite 17-51	0,0189	1,033	27,98	25,10	139,8	246,0
	0,0285	1,065	24,39	20,82	146,7	
	0,0406	1,083	22,05	18,01	154,0	
	0,0701	1,1	17,26	13,01	158,4	
Composite K-18-2	0,0659	1,45	36,63	37,21	109	20,8
	0,0910	1,42	34,02	34,12	110	
	0,122	1,38	30,15	29,65	111	
	0,327	1,36	26,57	25,56	112	
	0,775	1,35	18,93	16,82	115	

Writing the kinetic equation for the reactions under consideration in the form

$$\frac{dQ}{d\tau} \equiv \Delta H \frac{d\varphi}{d\tau} = \Delta H k_0 \exp\left(-\frac{F}{T}\right) (1-\varphi)^n, \quad (2)$$

we determined  $k_0$  (the pre-exponential factor),  $F$  (the index of the exponential), and  $n$  (the effective reaction parameter) in Arrhenius coordinates by analysis in the Promin<sup>1</sup>-2 computer, using as initial data the experimentally determined curve of the absorbed or liberated power, processed in accordance with Eq. (1), together with the sample-heating thermograph. The criterion for the choice of  $n$  was the linear relationship

$$\lg \left[ \frac{\frac{d\varphi}{d\tau}}{(1-\varphi)^n} \right] \text{ as a function of } 1/T, \text{ where } T \text{ is the temperature.}$$

The possibility of using Eq. (2) to describe the kinetics of heat evolution in certain chemically reacting materials was considered in [3].

Our kinetic curves based on the tabulated data agree with the experimental values (within the limits of experimental error), so justifying the use of Eq. (2) to describe the kinetic characteristics of the reactions taking place on heating the materials, as shown in Table 1.

By way of a trial problem, we determined the heats of fusion of chemically pure naphthalene and benzoic acid. Subject to stable reproducibility of the results of the measurements, the resultant heats of fusion differ by no more than 3% from the All-Union Scientific-Research Institute of Metrology Standard data. An analysis of the errors committed in determining the kinetic constants of the reactions showed that the principal errors lay in the calibration of the thermal-flux sensor, together with the recording and graphical analysis of the experimental results. The total error due to these factors was 4% or under.

Table 1 shows the results of a quantitative investigation into the thermal effects of the reactions involved in the hardening and vulcanization of certain materials.

We see from the table that the pre-exponential factor  $k_0$ , the effective reaction parameter  $n$ , and the exponential index  $F$  depend not only on the material studied, but also on the rate of heating. This dependence may be explained by the fact that for all the materials under consideration the reactions have a complex parallel-progressive character, in which particular stages of the reaction prevail over others in accordance with the temperature, which is itself uniquely related to the heating rate. The parameters so determined represent

effective, overall characteristics. The tendency for  $k_0$ ,  $F$ , and  $n$  to become independent of the heating rate on increasing the latter may be explained on the same general basis.

#### LITERATURE CITED

1. V. D. Moiseev, N. G. Avetisyan, A. G. Chernova, and A. A. Atruskevich, *Plast. Massy*, 12, No. 3 (1971).
2. E. Calvet and H. Prat, (editors), *Recent Progress in Microcalorimetry*, Pergamon (1963).
3. N. I. Basov, Yu. V. Kazankov, A. I. Leonov, V. A. Lyubortovich, and V. A. Mironov, *Izv. Vyssh. Uchebn. Zaved., Khim. Khim. Tekhnol.*, 12, No. 11 (1969).

#### A 2-MW HYDROGEN PLASMOTRON

R. Ya. Zakharkin, A. V. Pustogarov,  
and Yu. V. Kurochkin

UDC 533.9.07

An end-plane type plasmotron permitting generation of high-pressure high-temperature hydrogen flows with mean mass temperature from 2000 to 5000°K is considered.

The development of a number of projects in the fields of plasmochemistry and metallurgy requires the use of low-temperature hydrogen-plasma generators at a power level of 1-10 MW at operating times up to 100 h, with high efficiency with respect to transformation of electrical energy into flow thermal energy. The specifics of some technological processes demand important additional requirements in the generator: high hydrogen purity (absence of electrode material impurities), ability to vary temperature, flow rate, and pressure over wide ranges, reproducibility of parameters from operation to operation, and minimal parameter pulsation during operation.

Plasmotrons operating with air, nitrogen, and inert gases have been studied thoroughly, and their power level has been increased to 50 MW [1]. However, conversion of such plasmotrons to operation with hydrogen produces significant difficulties connected with the increase in energy liberation in the electrode regions [2] and decrease in stability of the arc discharge. Of existing hydrogen plasmotrons, those with power greater than 1 MW are of practical interest (Table 1).

The gas turbulence plasmotron of [3] has high efficiency and is capable of continuous operation for hundreds of hours. However, use of graphite electrode coatings leads to enrichment of the hydrogen plasma by carbon. In the operation of the coaxial hydrogen plasmotron of [2] the significant erosion of the central electrode limits operating time even with use of porous tungsten filling. Improvements of this method led to creation of plasmotrons with electrode gas curtains at places of arc contact, which allows generation of a flow of hydrogen-containing working plasma at pressures up to 50 atm. The end-plane type plasmotron allows combination of the advantages of the gas turbulence system (high efficiency) and the coaxial system (high pressure).

The present study will offer results of an experimental investigation of an end-plane type plasmotron with a power level of 2 MW.

#### 1. Plasmotron Operation

The plasmotron construction consists of a thermocathode formed of lanthanum-coated tungsten ( $V_L = 10$ ,  $d_C = 7-10$  mm,  $l_C = 70-120$  mm), soldered to a water-cooled copper nozzle, intermediate electrical insulation, and an anode ( $d_a = 20, 40, \text{ and } 74$  mm) with a solenoid mounted on it [4]. Figure 1 presents the volt-ampere characteristics and the mean mass hydrogen temperature of the plasmotron. Thermal efficiency is limited mainly by anode losses which increase linearly with current [5]. With an increase in the arc chamber diameter

---

Translated from *Inzhenerno-Fizicheskii Zhurnal*, Vol. 29, No. 6, pp. 1084-1090, December, 1975. Original article submitted December 25, 1974.

*This material is protected by copyright registered in the name of Plenum Publishing Corporation, 227 West 17th Street, New York, N.Y. 10011. No part of this publication may be reproduced, stored in a retrieval system, or transmitted, in any form or by any means, electronic, mechanical, photocopying, microfilming, recording or otherwise, without written permission of the publisher. A copy of this article is available from the publisher for \$7.50.*